








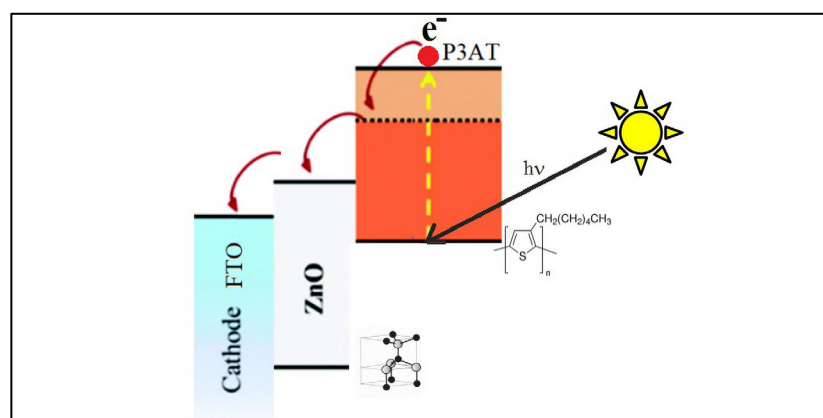
Full Paper | <http://dx.doi.org/10.17807/orbital.v13i2.1451>

Application of Zinc Oxide Nanospheres for Hybrid Solar Cell

Douglas Santos Oliveira ^a, Guilherme Arielo Rodrigues Maia ^b, Leticia Fernanda Gonçalves Larso ^a, Gideã Taques Tractz ^a, Henrique de Santana ^a, Sandra Regina Masetto Antunes ^c, and Paulo Rogério Pinto Rodrigues ^a

Poly(3-alkylthiophenes), P3AT, are organic polymers formed by conjugate structures with conductive properties. Zinc oxide (ZnO) has been used as an electron acceptor in hybrid solar cells because it offers electron transport properties and can be synthesized by methods in which the variation of synthesis parameters allows morphological control. Different ZnO morphologies allow for distinct properties in terms of electronic transport at the interface of solar cells. ZnO particles were synthesized by the co-precipitation method. ZnO films were deposited by spin-coating in Fluorine Tin Oxide (FTO) and then immersed in solutions containing poly (3-hexylthiophene) (P3HT) or poly (3-octylthiophene) (P3OT) polymers. The cell was assembled in the form of a sandwich consisting of: FTO/ZnO,P3AT/I⁻,I₃⁻/Pt/FTO. UV-vis measurements were performed for bandgap calculation, scanning electron microscopy (SEM), X-ray diffraction (XRD), and J-V curves. The ZnO/P3HT cell presented the best values of J, V and η , indicating an improvement in the electronic transfer processes, with a value of $\eta = 0.56\%$.

Graphical abstract



Keywords

Solar energy
Semiconductor
Polymer
Renewable energy

Article history

Received 08 January 2020
Revised 26 March 2021
Accepted 26 March 2021
Available online 20 June 2021

Handling Editor: Sergio R. Lázaro

1. Introduction

ZnO is a promising material for several applications due to its high optical transparency in the range of visible and electrical conductivity [4]. It is a metal oxide that has a range of applications such as ultraviolet radiation absorption [5],

^a Universidade Estadual do Centro, Campus Cedeteg, Departamento de Química, Rua Simeão Varela de Sá, 03, Vila Carli, Guarapuava-PR, Brazil. ^b Universidade Estadual de Londrina, Rodovia Celso Garcia Cid- Pr 445, Km 380, Londrina-PR, Brazil. ^c Universidade Estadual de Ponta Grossa, Avenida General Carlos Cavalcanti, 4748, Uvaranas, Ponta Grossa-PR, Brazil. *Corresponding author. E-mail: douglas.santos.oliver@gmail.com

photocatalyst [6,7], electronic devices [8], laser [9], transistors and solar cells [10-12]. It is an n-type intrinsic semiconductor presenting the crystalline structure in the hexagonal form of the wurtzite type (Figure 1a) [13] and has been used as an electron acceptor in hybrid solar cells since it offers electron transport properties, simple manufacturing techniques, variation and morphological control [14].

For the optoelectronic area, P3AT (Poly-3-alkylthiophene)

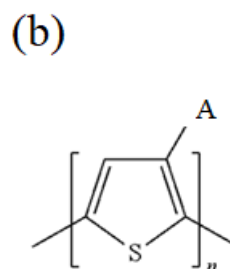
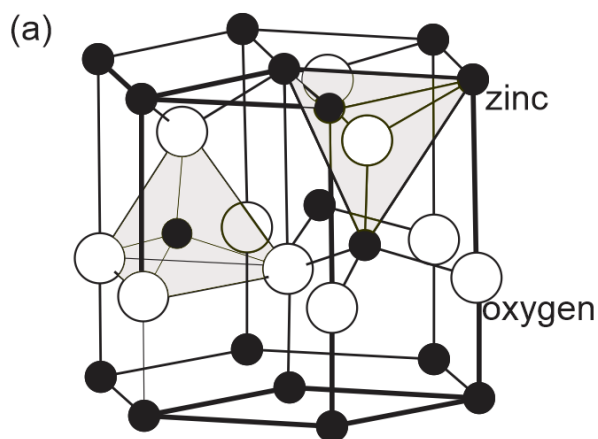


Fig. 1. (a) ZnO crystalline structure in the hexagonal form of the wurtzite type (adapted from [4]) and (b) chemical structure of poly (3-alkylthiophene), A = alkyl radical.

The operation of the solar cells starts when the device receives solar energy. Electrons in the polymer valence band are light excited to a high energy state (LUMO) and injected into the zinc oxide, conduction band, leaving holes in the polymer molecules. These holes are filled with iodine in (I⁻) present in the electrolyte, therefore, they are converted in I₃⁻. The electrons in the conduction band oxide travel through the external circuit, reaching the positive electrode, Cathode (CE). Finally, the electrolyte is regenerated by diffusion process in CE [22]. The electron injection mechanism from P3AT to ZnO is shown in Figure 2.

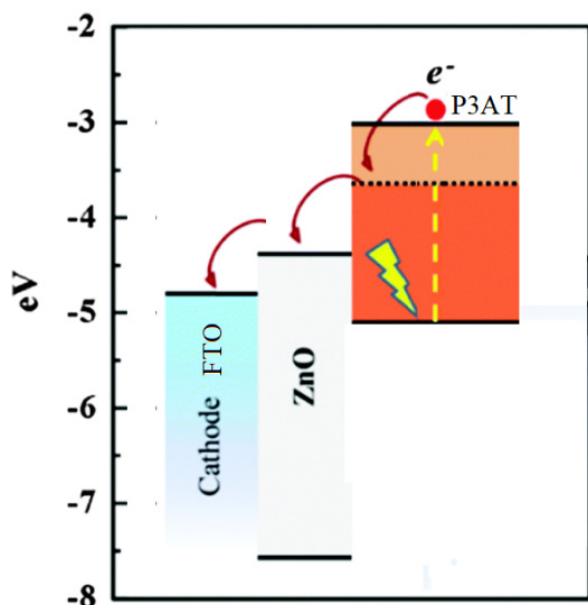


Fig. 2. Illustration of electron transition mechanism in cathode direction.

Thus the diagram for the solar cell can be described

(Figure 1b) has achieved great advances, considering that this compound is applied in organic light-emitting diodes (OLEDs), organic solar cells and low-cost integrated circuits [15-19], is highly photosensitive with sufficient absorption of visible light, which allows the use of this material as an optical absorber in photovoltaic cells [18,20,21] and the use of this material as an electron donor in hybrid solar cells has been increasing [14].

schematic representation of the cell according to IUPAC: FTO/ZnO,P3AT/ I₃⁻/Pt/FTO. High performance of these devices depends on optimizing the properties of the interfaces. Thus, interfaces with better properties in order to avoid or at least hinder electronic recombination losses that compromise device performance can be obtained by improving the properties of the materials that make up each interface. One of the properties to consider is the morphologies of ZnO. Thus, the objective of this work was applied nanospheres of ZnO in HSC composed of ZnO/P3OT and ZnO/P3HT

2. Material and Methods

ZnO particles were synthesized by co-precipitation method, using an aqueous solution of Zn(NO₃)₂·6H₂O and triethanolamine 0.1 mol L⁻¹. The mix was performed in a closed Erlenmeyer of 125 mL, to avoid the evaporation process. The solution was allowed to stand in 60 °C and 16 h. The produced powder was centrifugated at 4500 rpm of speed, and dried at 100 °C in an oven [14].

X-ray Diffraction (XRD)

X-ray diffraction was obtained by Bruker XRD D2 Phaser equipment, with 1.54 Å at 30 kV, 10 mA, and 0.5° s⁻¹ of scanning speed with LynEye detector. The Scherrer Equation was used to calculate the mean size of the crystallite (Equation 5), where d is the crystallite size (nm), K is the particle shaped constant (0.94), θ diffraction angle, β width at half height of diffraction peak, and γ is the radiation wavelength (1.54 Å).

$$d = K\gamma / (\beta \cos\theta) \quad (\text{Equation 5})$$

Scanning Electron Microscopy (SEM)

Scanning electron microscopy images were performed by TESCAN SEM VEGA 3 with SE detector and tungsten filament at 20 kV and 10 mm and 15 mm WD.

UV-Vis Spectra

UV-Vis spectra measurement for the ZnO films were performed on Shimadzu ultraviolet-visible spectrophotometer, model UV-2600 with wavelength range of 190 nm to 1100 nm.

ZnO films preparation

ZnO paste films (Working Electrode) were produced using 3 g of ZnO particles, 0.1 mL Triton X (Vetec), 0.1 mL acetyl acetone 99.5 % (Vetec), and 4 mL of ultrapure H₂O Milli-Q. For the first preparation stage, ZnO, acetylacetone, and 1 mL of H₂O were mixed for 40 minutes. In a second step, Triton X and the remaining 3 mL of H₂O were added and paste was kept under maceration for 10 minutes [14,23].

The deposition was performed in transparent conductor glass of fluorine tin oxide (FTO~7Ω sq⁻¹) by the spin-coating method, in 3000 rpm for 30 seconds. It was coated 0.2 mL of the ZnO paste in FTO glass, and it was heated at 450 °C for 30 minutes to burning the organic matter.

The produced films were sensitized using poly (3-hexylthiofeno) (P3HT) e poly (3-octylthiofeno) (P3OT). The conductor polymers were provided by the Spectroscopy Laboratory from UEL (LabSPEC). The polymers solutions were prepared using toluene as solvent according to Machado [24]. ZnO films were immersed in the polymeric solutions for 24 h.

Platinum counter electrode

For the production of the Pt counter electrode, a solution of 8 mmol L⁻¹ of K₂PtCl₆ in 0.1 mol L⁻¹ HCl was prepared. The platinum was electrodeposited by cyclic voltammetry in five cycles in FTO, with a potential range of -0.5 V and a sweep speed of 20 mV s⁻¹.

Iodide/triiodide electrolyte

The electrolyte was prepared with iodide/triiodide (I⁻/I₃⁻) redox couple, which consists of a solution of ethylene glycol with 0.5 mol L⁻¹ Lil and res sublimated iodine (I₂) 0.5 mol L⁻¹.

Solar Cell assemble

The Solar cell was assembled in the sandwich format of an anode (FTO/ZnO/P3OT or P3HT) and a cathode (FTO/Pt) in contact with the electrolyte in the active area of 0.2 cm².

3. Results and Discussion

X-ray diffraction (XRD) presented in Figure 3 was performed to investigate the crystal phase.

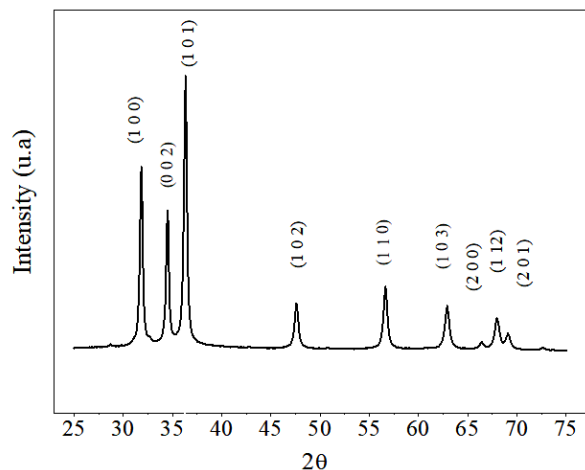


Fig. 3. X-ray diffractogram for ZnO particles.

The XRD result (Figure 3) indicated of the ZnO presented wurtzite crystalline structure according to the crystallographic form PDF 01-075-0576 [25], which represents a unit cell in the compact hexagonal system characteristic of ZnO. Using the Scherrer equation (1918) [26], it was calculated the crystallite size, which has an average size of 19.95 nm, compatible with the values found in the literature, which presents the range between 10-50 nm [27]. The sample showed 82.4% of crystallinity, free of high concentrations of impurities, and secondary peaks were not detected.

The Figure 4 presents the SEM images to ZnO.

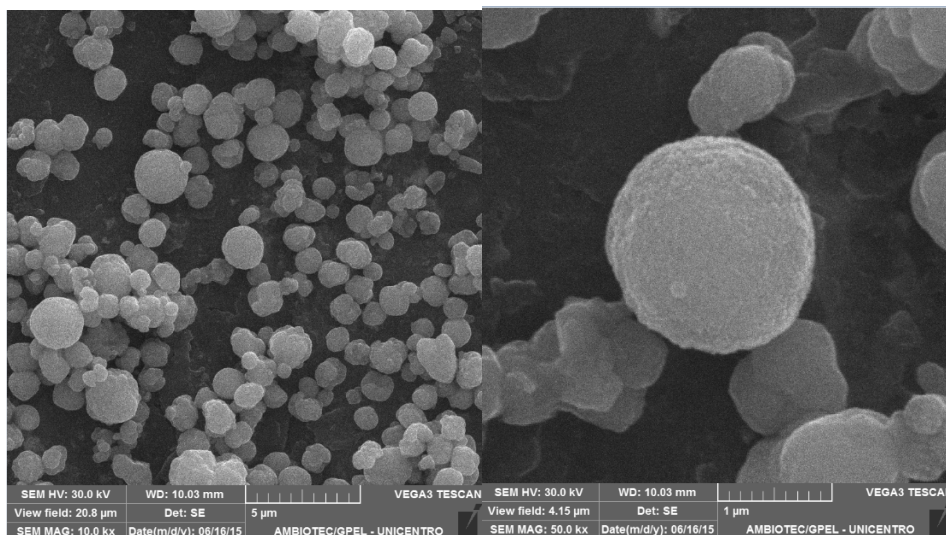


Fig. 4. SEM images for ZnO particles.

According to Maia et al. [14] and Zhao et al. [28], ZnO is a positive pole crystal (Zn^{2+}) and a negative pole (O^{2-}), when the molar ratio is 1:7.5 the particles seek to minimize surface energy, and thus the formed nanoparticles rearrange on the surface of the ZnO nuclei, so that the nanostructures became

sphere-shaped.

Figure 5a shows the absorbance spectra in the UV-Vis region by reflectance and 5b shows the curves $(\alpha h\nu)^2$ as a function of E (eV) for ZnO films.

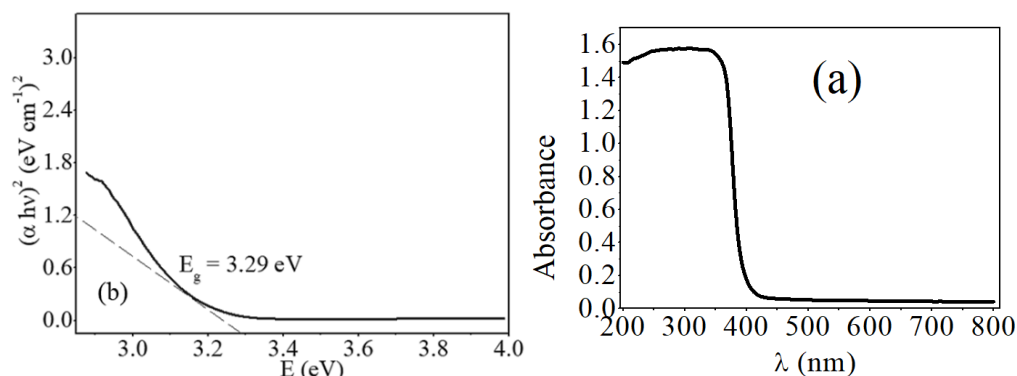


Fig. 5. UV-vis spectrum (a) and bandgap of ZnO (b) nanospheres.

Optical absorption measurements provide an estimate of energy and indicate about the nature of the electronic transition of a semiconductor. Through optical absorption data, it was possible to determine the absorption coefficient (α), using the film thickness Floriano et al. [29]. The absorption coefficient α was determined by Equation 1, from the result of absorbance (A) and thickness (L) measurements of the films.

$$\alpha = \frac{2.303 A}{L} \text{ (Equation 1)}$$

Scanning electron microscopy results of the cross-section indicated that the film thickness averaged $28.00 \pm 5 \mu\text{m}$. With the value of the absorption coefficient α , the material bandgap was estimated by Equation 2 of the Tauc method [30].

$$(\alpha h\nu) = B(h\nu - E_g)^y \text{ (Equation 2)}$$

α = absorption coefficient;

B = constant;

h = Planck constant = $4.4 \times 10^{-15} \text{ eV s}$;

ν = frequency of incident radiation;

E_g = bandgap (eV);

y = constant of semiconductor transition.

The y value defines the type of transition, where y can assume the values of $1/2$, $3/2$, 1 , 2 , and 3 , depending on the nature of the material's bandgap. If the nature of the material's electronic transition is straightforward, the extrapolation of the curve $(\alpha h\nu)^2$ as a function of the incident photon energy to the zero ordinate value gives an estimate of the bandgap energy. On the other hand, if the nature of the material's electronic transition is of the indirect type, the extrapolation of the curve $(\alpha h\nu)^{1/2}$ as a function of the incident photon energy to the zero ordinate value gives an estimate of the bandgap energy [31]. According to Trindade et al. [30], ZnO has a direct transition (or gap) and the gap estimate using this method has presented results more consistent with the expected and the most used by several

researchers [32-34].

ZnO bandgap was calculated, assuming that the transition between bands was a direct one. The value found by extrapolating the linear region of the curve $(\alpha h\nu)^2$ to the zero value of the ordinate was 3.29 eV. The bandgap values found are similar to Klubnuan et al. [35], with the ZnO film in nano plaques and lamellas morphologies present values of 3.23 and 3.22 eV respectively. For Rokhsat and Akhavan [36] ZnO films with nanotube morphology have bandgap values of 3.24 eV.

Figure 6 shows the j - V curves for all cells studied.

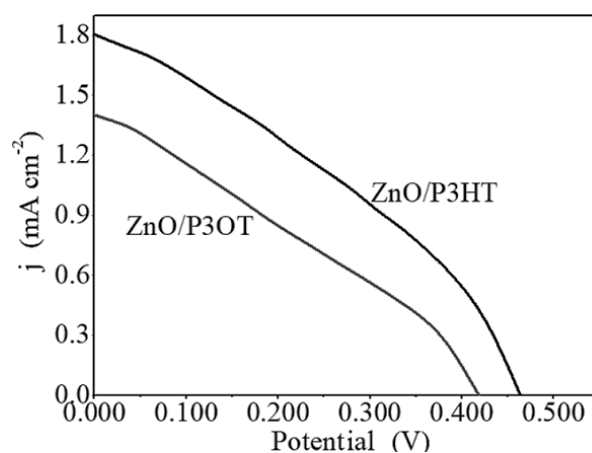


Fig. 6. j - V curves to cell produced of ZnO/P3OT and ZnO/P3HT.

When the voltage applied to the cell terminals is zero, the current produced by the cell reaches its maximum, as can be seen from Figure 6, where the samples ZnO/P3HT and ZnO/P3OT presented those of J_{sc} (short circuit photocurrent), being 1.80 and 1.41 mA cm^{-2} , respectively. The current is associated with the electron injection mechanism and the charge transport of the carriers. There is a significant increase in photocurrent density (J_{sc}) and a decrease in open circuit potential for P3HT cells compared to P3OT.

The FF (fill factor) and η values were obtained using

Equation 3 and 4 respectively, where I_{mp} and V_{mp} is the current density and potential of the j-V curve at the maximum [14]. The FF is the ratio between the ideal maximum power and the real experimental power, obtained from the cell, η represents the efficiency of the cell and demonstrates the relationship between the energy power, that reaches the cell and the electrical values produced by it [37].

$$FF = \frac{I_{mp}V_{mp}}{J_{sc}V_{oc}} \text{ (Equation 3)}$$

$$\eta = \frac{J_{sc}V_{oc}FF}{P_{in}} \cdot 100\% \text{ (Equation 4)}$$

The parameters J_{sc} and V_{max} presented in Table 1 correspond respectively, the current and voltage density at the maximum output power of the cell, $P_{max} = J_{sc} \cdot V_{max}$. The values of V_{oc} (Open circuit potential) were obtained when $J = 0$, while, J_{sc} , was obtained with $V = 0$.

Table 1. Parameters (for 100 mW cm⁻² illumination) obtained by the j-V curves of hybrid solar cells.

HSC	J_{sc} / mA cm ⁻²	P_{max} / mW	V_{max} / V	FF	η / %
ZnO/P3HT	1.80	0.83	-0.463	0.337	0.56
ZnO/P3OT	1.41	0.59	-0.419	0.335	0.38

It is also noted a higher efficiency in energy conversion, to P3HT sensitized cell, and it can be suggested by the better charge injection, producing a solar cell with $\eta = 0.56\%$. The values shown are satisfactory when compared to the literature results, using ZnO synthesized by electrochemical hydrothermal method, with nanorods morphology, which presents maximum parameters of $J_{sc} = 1.21$ mA cm⁻², $V_{max} = 0.59$ V. $FF = 0.48$ e $\eta = 0.34\%$ [38].

4. Conclusions

It was possible to produce and apply the ZnO nanospheres in conducting polymer solar cells. XRD confirmed the formation of zinc oxide of wurtzite crystalline structure, with high purity and SEM images showed that the synthesized oxide acquired spherical morphology.

The devices studied presented significant results to the conversion of solar energy to electricity and satisfactory to these classes of cells, showing maximum η of 0.56% for the ZnO/P3HT cell. The ZnO/P3HT photovoltaic system presented higher photoelectrochemical parameters, indicating a better electronic charge transfer process.

Acknowledgments

This study was financed in part by the Coordenação de Aperfeiçoamento de Pessoal de Nível Superior – Brazil (CAPES) – Finance Code 001.

Author Contributions

Conceptualization, Guilherme Arielo Rodrigues Maia; Methodology, Gideã Taques Tractz; Guilherme Arielo Rodrigues Maia; Leticia Fernanda Gonçalves Larsson. Investigation, Gideã Taques Tractz; Douglas Santos Oliveira; Guilherme Arielo Rodrigues Maia; Leticia Fernanda

Gonçalves Larsson. Resources, Paulo Rogério Pinto Rodrigues; Henrique de Santana. Data curation, Guilherme Arielo Rodrigues Maia; Leticia Fernanda Gonçalves Larsson; Gideã Taques Tractz. Writing—original draft preparation, Writing—review and editing, Sandra Regina Masetto Antunes; Gideã Taques Tractz; Douglas Santos Oliveira; Guilherme Arielo Rodrigues Maia, Paulo Rogério Pinto Rodrigues; Supervision, Sandra Regina Masetto Antunes; Paulo Rogério Pinto Rodrigues.; Project administration, Paulo Rogério Pinto Rodrigues.; All authors have read and agreed to the published version of the manuscript.

References and Notes

- [1] Hassan, N. K.; Hashim, M. R.; Al-Douri, Y. *Optik*. **2014**, *125*, 2560. [\[Crossref\]](#)
- [2] Ikram, M.; Imran, M.; Nunzi, J. M.; Ali, S. J. *Mater. Sci. Mater. Electron.* **2015**, *26*, 6478. [\[Crossref\]](#)
- [3] Thanihaichelvan, M.; Sockiah, K.; Balashangar, K.; Ravirajan, P. *J. Mater. Sci. Mater. Electron.* **2015**, *26*, 3558. [\[Crossref\]](#)
- [4] Mayrinck, C.; Raphael, E.; Ferrari, J. L.; Schiavon, M. A. *Rev. Virtual Quim.* **2014**, *6*, 1185. [\[Crossref\]](#)
- [5] Yuan, Z.; Fu, M.; Ren, Y.; Jiang, Y.; Wu, Z. *J. Mater. Sci. Mater. Electron.* **2015**, *26*, 8212. [\[Crossref\]](#)
- [6] An, S.; Joshi, B. N.; Lee, M. W.; Kim, N. Y.; Yoon, S. S. *Appl. Surf. Sci.* **2014**, *294*, 24. [\[Crossref\]](#)
- [7] Hsu, N. F.; Chang, M.; Hsu, K. T. *Mater. Sci. Semicond. Process.* **2014**, *21*, 200. [\[Crossref\]](#)
- [8] Broitman, E.; Soomro, M. Y.; Lu, J.; Willander, M.; Hultman, L. *Phys. Chem. Chem. Phys.* **2013**, *15*, 11113. [\[Crossref\]](#)
- [9] Huang, M. H. *Science Adv.* **2001**, *292*, 1897. [\[Crossref\]](#)
- [10] Yuan, Z.; Fu, M.; Huang, W. *Synth. Met.* **2013**, *185-186*, 133. [\[Crossref\]](#)
- [11] Seow, Z. L. S.; Wong, A. S. W.; Thavasi, V.; Jose, R.; Ramakrishna, S.; Ho, G. W. *Nanotechnology* **2009**, *20*, 045604. [\[Crossref\]](#)
- [12] Belaid, H.; Nouri, M.; Ayadi, Z. B.; Djessas, K.; El Mir, L. *J. Mater. Sci. Mater. Electron.* **2015**, *26*, 8272. [\[Crossref\]](#)
- [13] Chen, C. T.; Hsu, F. C.; Kuan, S. W.; Chen, Y. F. *Sol. Energy Mater. Sol. Cells.* **2011**, *95*, 740. [\[Crossref\]](#)
- [14] Maia, G. A. R.; Larsson, L. F. G.; Viomar, A.; Matos, L. A. C.; Antunes, S. R. M.; Maia, E. C. R.; Oliveira, M. F.; Cunha, M. T.; Rodrigues, P. R. P. *J. Mater. Sci. Mater. Electron.* **2016**, *27*, 8271. [\[Crossref\]](#)
- [15] Singh, B.; Alloway, B. J.; Bocheureau, F. J. M. *Commun. Soil Sci. Plant Anal.* **2000**, *31*, 2775. [\[Crossref\]](#)
- [16] Qi, Z. Jian; Feng, W. D.; Sun, Y. M.; Yan, D. Z.; He, Y. F.; Yu, J. J. *J. Mater. Sci. Mater. Electron.* **2007**, *18*, 869. [\[Crossref\]](#)
- [17] Bento, D. C.; Maia, E. C. R.; Rodrigues, P. R. P.; Moore, G. J.; Louarn, G.; De Santana, H. *J. Mater. Sci. Mater. Electron.* **2013**, *24*, 4732. [\[Crossref\]](#)
- [18] Kim, C. H.; Kisiel, K.; Jung, J.; Ulanski, J.; Tondelier, D.; Geffroy, B.; Bonnassieux, Y.; Horowitz, G. *Synth. Met.* **2012**, *162*, 460. [\[Crossref\]](#)
- [19] De Santana, H.; Maia, E. C. R.; Bento, D. C.; Cervantes,

- T. N. M.; Moore, G. J. *J. Mater. Sci. Mater. Electron.* **2013**, *24*, 3352. [\[Crossref\]](#)
- [20] Vanlaeke, P.; Swinnen, A.; Haeldermans, I.; Vanhoyland, G.; Aernouts, T.; Cheyns, D.; Deibel, C.; D'Haen, J.; Heremans, P.; Poortmans, J.; Manca, J. V. *Sol. Energy Mater. Sol. Cells* **2006**, *90*, 2150. [\[Crossref\]](#)
- [21] Mihailetchi, V. D.; Xie, H.; De Boer, B.; Koster, L. J. A.; Blom, P. W. M. *Adv. Funct. Mater.* **2006**, *16*, 699. [\[Crossref\]](#)
- [22] Agnaldo, J. S.; Bastos, J. B. V.; Cressoni, J. C.; Viswanathan, G. M. *Rev. Bras. Ens. Fis.* **2006**, *28*, 77. [\[Crossref\]](#)
- [23] Parussolo, A. L. A.; Iglesias, B. A.; Toma, H. E.; Araki K. *Chem. Commun.*, **2012**, 48. 6939. [\[Crossref\]](#)
- [24] Machado, W. S. Memórias orgânicas baseadas em esferas de carbono e transistores de efeito de campo orgânicos e baixa tensão de operação. [Doctoral dissertation.] Curitiba, Brazil: Universidade Federal do Paraná, PPGFís, 2011. [\[Link\]](#)
- [25] Pookmanee, P.; Makarunkamol, S.; Satienperakul, S.; Kitikul, J.; Phanichphant, S. *Adv. Mat. Res.* **2010**, *93-94*, 643. [\[Crossref\]](#)
- [26] Kroon, R. S. *Afr. J. Sci.* **2013**, *109*, 5. [\[Crossref\]](#)
- [27] Silva, S. S.; Magalhães, F.; Sansiviero, M. T. C. *Quim. Nova.* **2010**, *33*, 85. [\[Crossref\]](#)
- [28] Zhao, X.; Li, M.; Lou, X. *Advan. Powd. Tec.* **2013**, *25*, 372. [\[Crossref\]](#)
- [29] Floriano, E. A.; Scalvi, L. V.; Sambrano, J. R. *Cêramica* **2009**, *55*, 88. [\[Link\]](#)
- [30] Trindade, N. M. Investigação das propriedades ópticas de ZnO e ZnO:Al. [Doctoral dissertation.] Sorocaba, Brazil: Universidade Estadual Paulista, 2015. [\[Link\]](#)
- [31] Sundaram, K. B.; Bhagavat, G. K. *J. Phys. D.* **1981**, *14*, 92. [\[Crossref\]](#)
- [32] Bensaha, R.; Bensouyad, H. In: *Heat Treat.: Conv. Novel Appl.* Czerwinski, F., ed. London: IntechOpen, 2012, Chapter 10. [\[Link\]](#)
- [33] Bisht, D.; Yadav, S. K.; Darmwal, N. S. *Braz. J. Microb.* **2013**, *44*, 1,245. [\[Crossref\]](#)
- [34] Sarm, D.; Das, T. M.; Barua, S. *J. Eng. Techn.* **2016**, *4*, 216. [\[Link\]](#)
- [35] Klubnun, S.; Suwanboon, S.; Amornpitoksuk, P. *Opt. Mat.* **2016**, *53*, 131. [\[Crossref\]](#)
- [36] Rokhsat, E.; Akhavan, O. *Appl. Surf. Sci.* **2016**, *371*, 590. [\[Crossref\]](#)
- [37] Freitas, J. N. Células fotovoltaicas híbridas de polímeros condutores e nanopartículas inorgânicas. [Doctoral dissertation.] Campinas, Brazil: Universidade Estadual de Campinas, 2009. [\[Link\]](#)
- [38] Fonseca, A. F. V.; Siqueira, R. L.; Landers, R.; Ferrari, J. L.; Marana, N. L.; Sambrano, J. R.; La Porta, F. A.; Schiavon, M. A. *J. Alloys Compd.* **2018**, *739*, 939. [\[Crossref\]](#)

How to cite this article

Oliveira, D. S.; Maia, G. A. R.; Larso, L. F. G.; Tractz, G. T.; Santana, H.; Antunes, S. R. M.; Rodrigues, P. R. *P. Orbital: Electron. J. Chem.* **2021**, *13*, 102. DOI: <http://dx.doi.org/10.17807/orbital.v13i2.1451>